Paper No. 1795. (quote when citing this article)
Eleventh World Conference on Earthquake Engineering
ISBN: 0 08 042822 3

SIMULATION ANALYSES OF FORCED VIBRATION TESTS ON BOTH HORIZONTAL AND VERTICAL EXCITATION OF PWR TYPE REACTOR BUILDING

M. SHIOTA, Y. SONO, J. AKASHI,
Kyushu Electric Power Co., Inc., Civil Engineering Department
2-1-82, Watanabe-dori, Chuou-ku, Fukuoka 810-91, JAPAN

Y. YASUI, M. KANEKO, M. OHORI,
Obayashi Corporation, Technical Research Institute
4-640, Shimo-Kiyoto, Kiyose, Tokyo 204, JAPAN

T. KUNO, Y. KOMATSU, M. ENDO
Obayashi Corporation, Nuclear Facilities Division
3-7, Nishi-Shinjuku, Shinjuku-ku, Tokyo 163-10, JAPAN

ABSTRACT

Many studies have been done for horizontal responses of reactor buildings using results of forced vibration tests. However, thorough study has not been done for vertical responses. In this paper, forced vibration tests and simulation analyses of tests are reported on both horizontal and vertical excitation of a Pressurized Water Reactor (PWR) type 4-loop reactor building (1,180 MWe), Genkai Nuclear Power Station Unit 3 of Kyushu Electric Power Co., Inc. From forced vibration tests, vibration characteristics such as natural frequency, modal shape, and modal damping factor of the reactor building were obtained. To simulate results of tests in detail, three-dimensional (3-D) FEM modeling was used. Results of analyses showed good agreement with those of tests with respect to vertical responses as well as horizontal responses. Through this study, it is confirmed that 3-D FEM modeling is an effective method to express vibration characteristics of the reactor building accurately.

KEYWORDS

Forced vibration tests, PWR type reactor building, Natural frequency, Damping factor, Modal shape, Vibration generator, Simulation analyses, 3-D FEM modeling, Resonance curve, Phase lag curve

FORCED VIBRATION TESTS

Outline of tests

The reactor building, which was the object of vibration tests, was a structure composed of a prestressed concrete containment vessel (PCCV), an inner concrete structure (I/C), and a reactor external building (RE/B), all built on the same base mat (B/M) with thickness of 9.8 m. An outline of the reactor building is shown in Fig.1.

I/C excitation and PCCV excitation were conducted separately. First, I/C excitation tests were performed in September and October 1992. A vibration generator was installed in operating floor of I/C (EL+11.3m) for I/C excitation of three directions (north-south, east-west, and vertical excitation). Second, PCCV excitation

test was performed in January and February 1993. A vibration generator was installed in the top of PCCV (EL+60.4m) for PCCV excitation of one direction (north-south). At both times, construction of the plant was almost completed and equipments were installed. For I/C excitation, tests were performed with frequency changing step by step between 1 Hz and 30 Hz. The maximum applied force was 10 t in horizontal excitation and 5 t in vertical excitation. For PCCV excitation, test was performed with frequency changing step by step between 1 Hz and 20 Hz. The maximum applied force was 2.5 t in PCCV excitation.

Basically, main purpose of I/C excitation was to obtain the vibration characteristics of I/C, but measurements were made not only in I/C but also in PCCV, RE/B and B/M to understand dynamic behavior as a whole building. In Fig.1, a sample of seismometers distribution is indicated with the solid circle (●). The number of total seismometers sums to 95 in horizontal case and 36 in vertical case, respectively. As for PCCV excitation, measurements were made in PCCV and B/M to obtain the beam and oval vibration characteristics of PCCV. The number of total seismometers sums to 39 in this case.

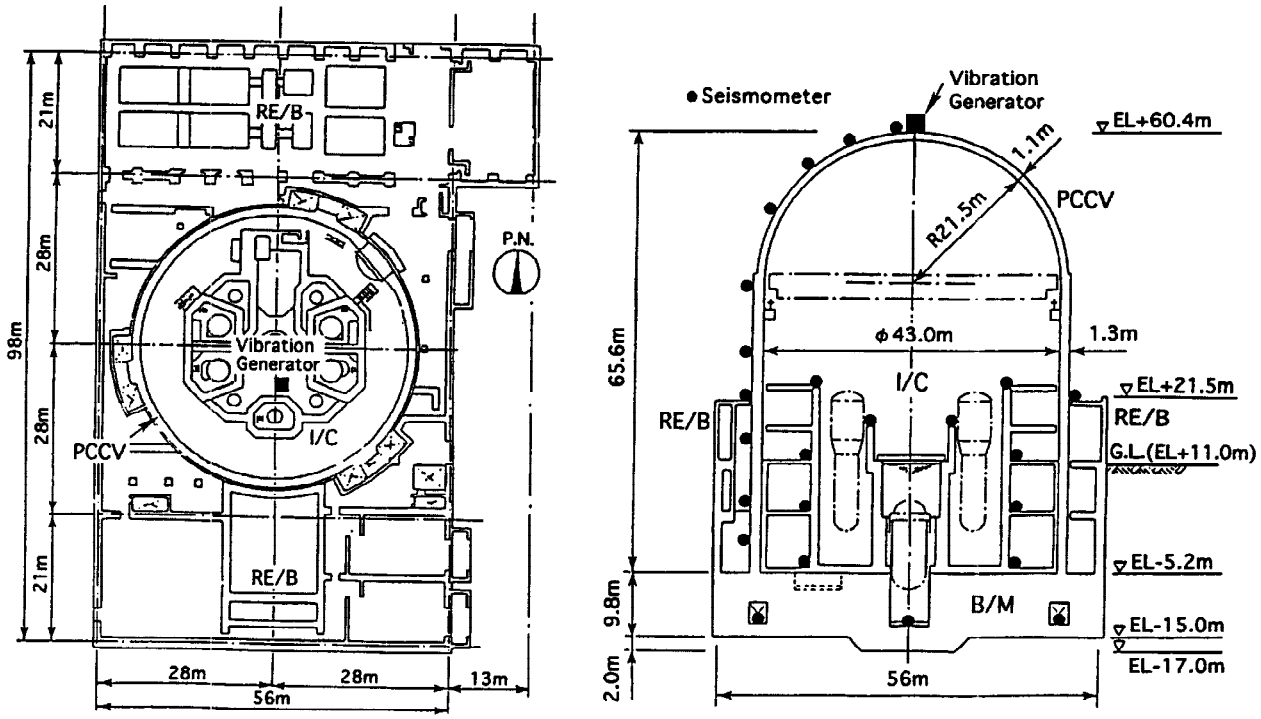

(a) Plan at EL+11.3m

(b) EW section (left: west, right: east)

Fig.1. Outline of the reactor building.

Results of tests

For I/C horizontal excitation, remarkable differences in vibration characteristics were not found between results of NS (north-south) directoin and EW (east-west) direction, so the following discussion focuses on results of NS direction. In Fig.2, representative examples of resonance curves and phase lag curves obtained from I/C excitation are shown. The open circle (○) in Fig.2(a) represents results of the top of PCCV (EL+60.4m) . The open circle (○) and the open triangle (△) in Fig.2(b) represent results of south side and north side of the operating floor of I/C (EL+11.3m). In resonance curves, the displacement amplitude is normalized for 1 ton of exciting force. In Fig.2(a), predominant frequencies of PCCV appear at 5.0 Hz , 9.65 Hz, and 15.3 Hz. In Fig.2(b), predominant frequency of I/C appears at 9.65 Hz. In Fig.3, modal shapes of PCCV and I/C are drawn at each predominant frequency, 5.0 Hz and 9.65 Hz, respectively. From Fig.3(a) and Fig.3(b), modal shapes are recognized as 1st mode of beam vibration of

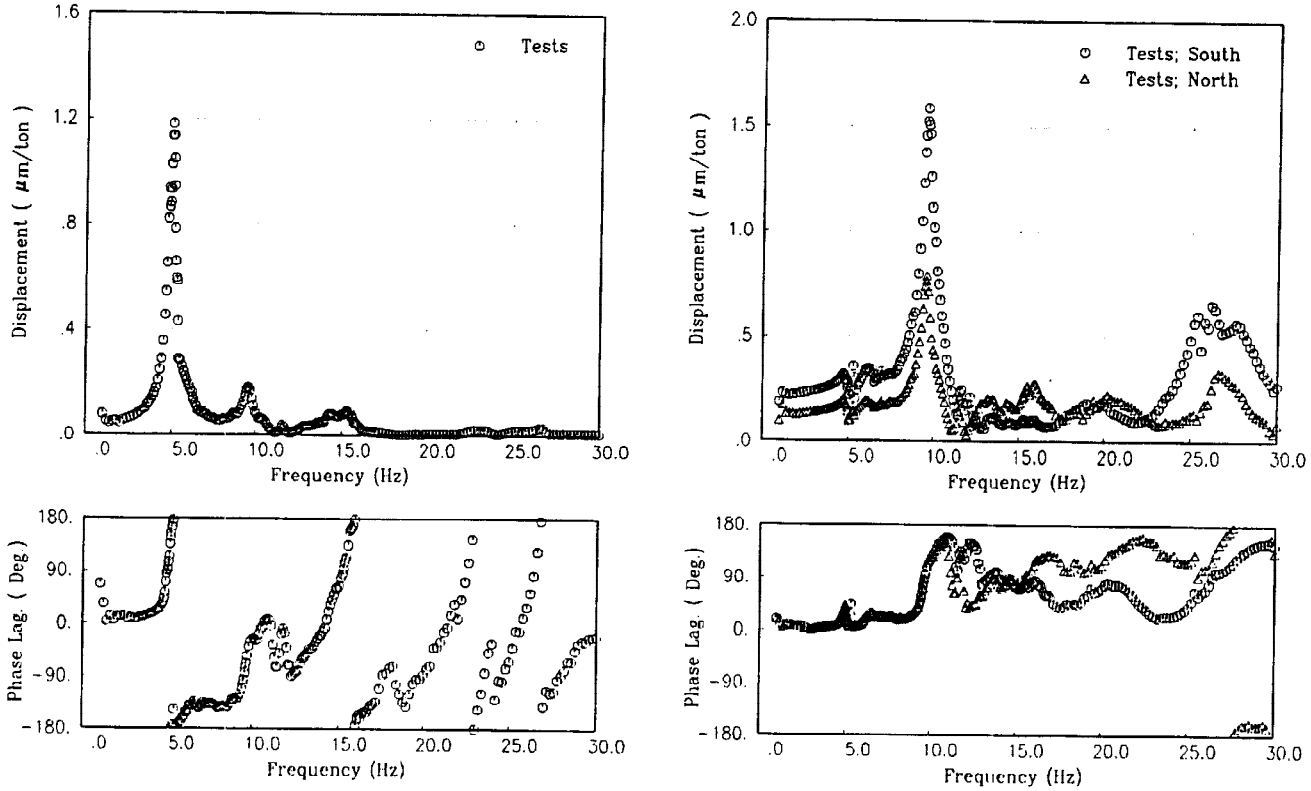

(a) PCCV (b) I/C

Fig.2. Resonance curves and phase lag curves from tests of I/C NS excitation.

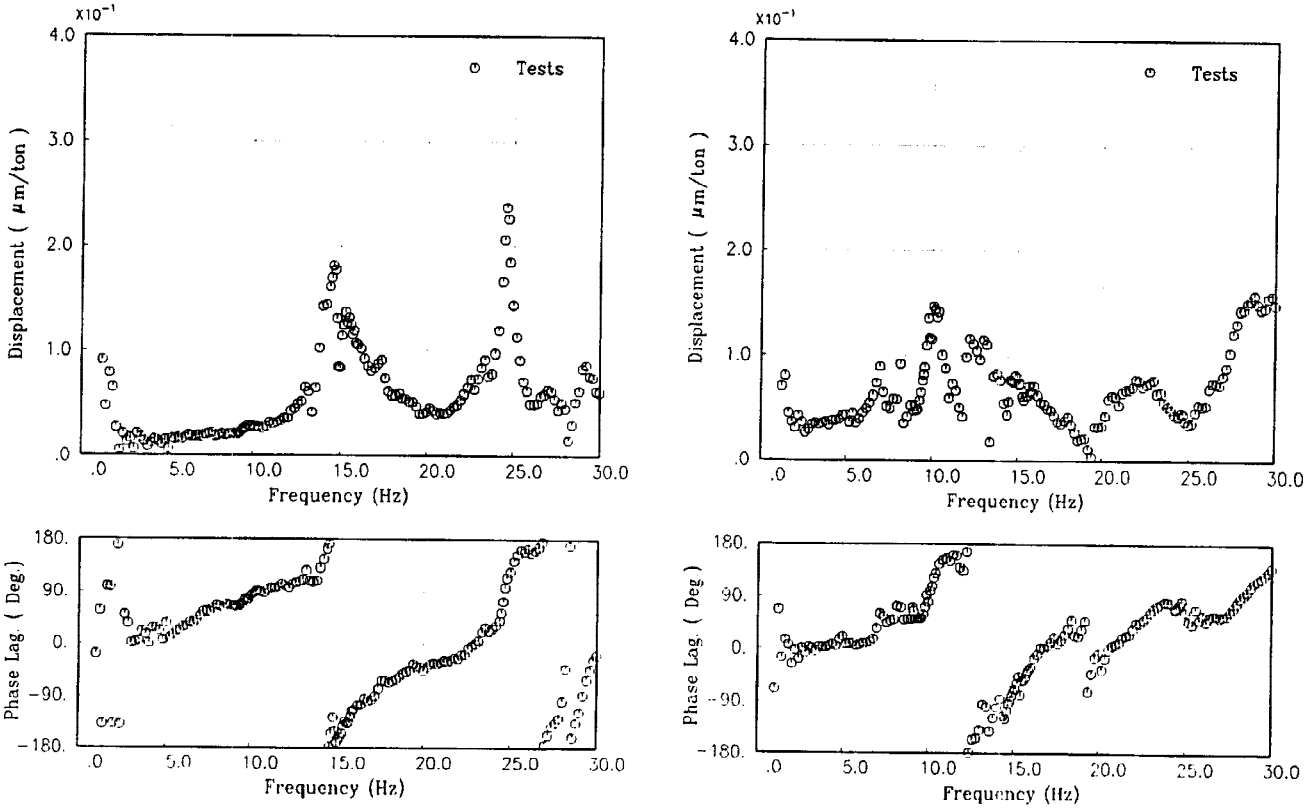

(a) PCCV (b) I/C

Fig.4. Resonance curves and phase lag curves from tests of I/C vertical excitation.

PCCV and I/C. Similarly, modal shape of PCCV at 15.3 Hz is recognized as 2nd mode of PCCV. Predominant frequency of PCCV at 9.65 Hz in Fig.2(a) seems to be induced by the influence of I/C 1st mode. Natural frequencies and damping factors from I/C excitation tests were determined by regression analyses as shown in Table 1.

For I/C vertical excitation, a representative example of resonance curves and phase lag curves are shown in Fig.4. Results of the top of PCCV (EL+60.4m) are shown in Fig.4(a) and results of south side of the operating floor of I/C (EL+11.3m) are shown in Fig.4(b). In Fig.4(a), predominant frequencies of PCCV appear at 14.6 Hz and 24.6 Hz. In Fig.4(b), predominant frequencies of I/C appear at 10.1 Hz, about 13 Hz, about 23 Hz, and about 29 Hz. By reference to results at other positions of PCCV, predominant frequencies at 14.6 Hz and 24.6 Hz in Fig.4(a) are regarded as 1st mode and 2nd modes of PCCV axial vibration (see Table 1). As for predominant frequencies of I/C, it is difficult to identify the vibration mode because predominant frequency depends on the position in I/C.

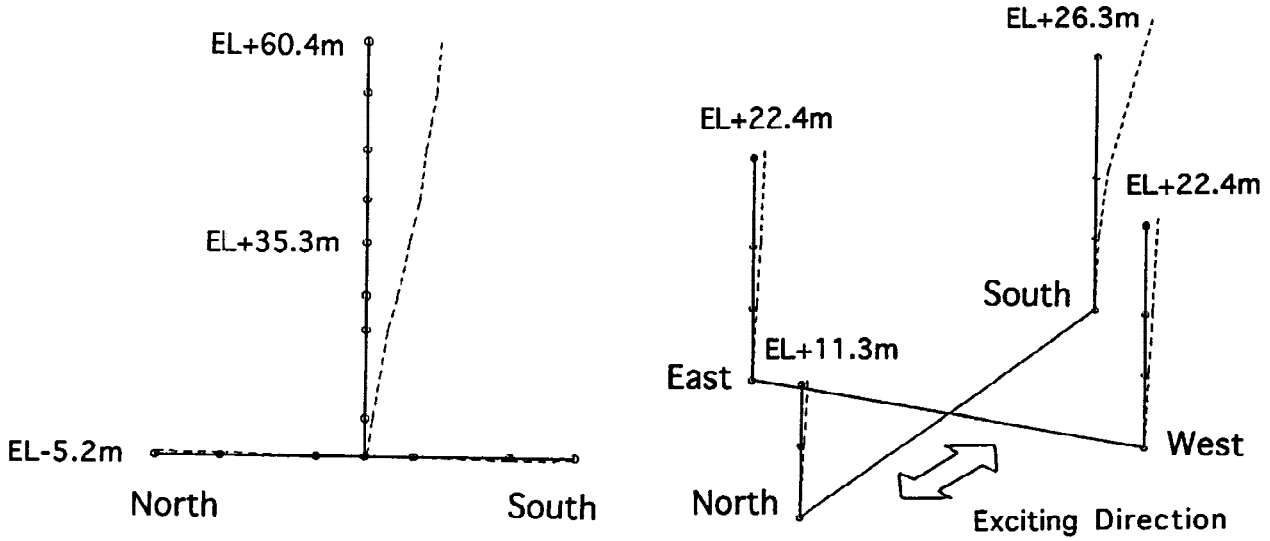

(a) PCCV (5.0 Hz)

(b) I/C (9.65 Hz)

Fig.3. Modal shapes of beam vibration from tests of I/C NS excitation.

Table 1. Natural frequencies and modal damping factors obtained from I/C excitation.

Direction	Mode	Natural Frequency	Damping Factor
NS	PCCV beam 1st	5.01 Hz	2.2 %
	I/C beam 1st	9.62 Hz	3.0 %
EW	PCCV beam 1st	4.73 Hz	1.8 %
	I/C beam 1st	9.71 Hz	3.8 %
UD	PCCV axial 1st	14.6 Hz	—

For PCCV NS excitation, measurements were made for oval vibration mode as well as beam vibration mode. Fig.5 shows results of modal shape measured at the wall of PCCV (EL+21.5m). These modal shapes correspond to beam 1st mode in Fig.5(a), oval mode (n=3) in Fig.5(b), and oval mode (n=2) in Fig.5(c). The other modal shapes were also obtained. Vibration characteristics of PCCV excitation are shown in Table 2. Aside from simulation analyses in the following section, preparatory analyses of eigenvalue problem of PCCV had been done using fully 3-D FEM model of PCCV with its bottom fixed.

In Fig.6, results from analyses marked with the open circle (○) are compared with those from tests marked with the solid circle (●). From this figure, good agreement is found between both results. In eigen value analyses, material properties in Table 3 were used.

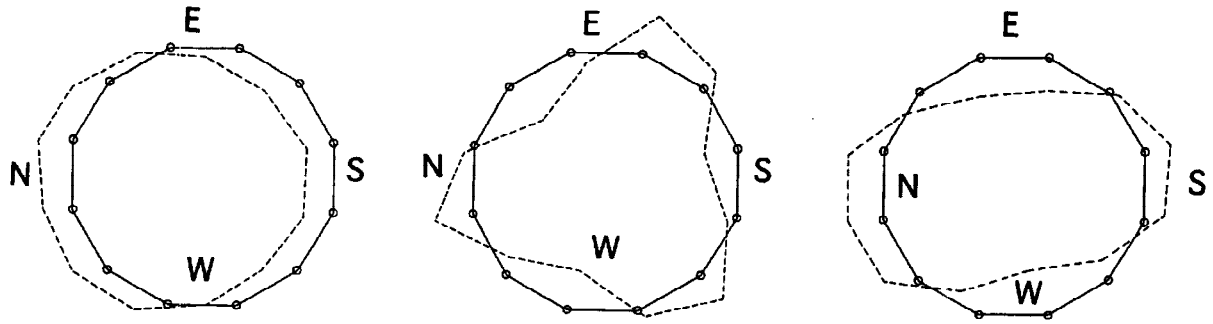

(a) 5.0 Hz (b) 7.9 Hz (c) 8.6 Hz

Fig.5. Modal shapes of oval vibration from tests of PCCV excitation.

Table 2. Natural frequencies and modal damping factors obtained from PCCV excitation.

Mode	Natural Frequency	Damping Factor
PCCV beam 1st (NS)	4.97* Hz	2.6* %
PCCV oval (n=3)	7.9 Hz	—
PCCV oval (n=2)	8.6 Hz	—
PCCV oval (n=4)	10.3 Hz	—
PCCV oval (n=5)	14.5 Hz	—
PCCV beam 2nd (NS)	14.87* Hz	1.9* %

[Note] Value with star (*) was obtained from regression analyses.

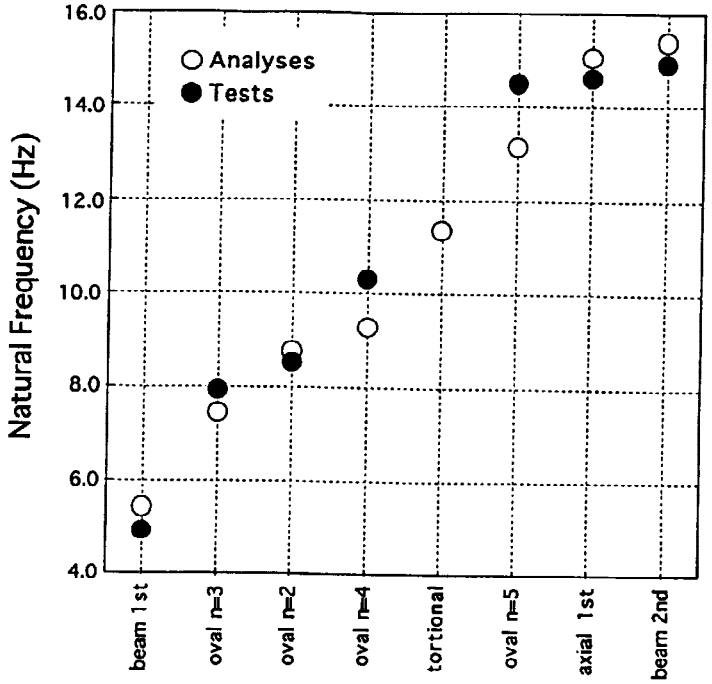

Fig.6. Natural frequencies of PCCV from tests of PCCV excitation.

SIMULATION ANALYSES

Modeling of 3-D FEM

To express the vibration characteristics of the reactor building in detail, 3-D FEM modeling was done. The outline of 3-D FEM model is shown in Fig.7. As seen in Fig.1, the shape of the reactor building is almost symmetrical with respect to NS axis. Therefore, in modeling of 3-D FEM, the assumption of symmetry of the building to NS axis was adopted and half degrees of freedom was reduced.

3-D FEM model consists of 1593 nodes and 1692 elements. Elements used here are classified into three types, 953 shell elements, 147 beam elements, and 592 solid elements. The length of each element is set to within one-sixth of the minimum wavelength in simulation analyses. To model the soil of half-space spreading out under the bottom of B/M, the thin layer elements were used with the bottom boundary connected to the viscous damper at a depth of 200 m.

In parallel with forced vibration tests, static and dynamic tests using concrete specimens were done. Field tests on elastic wave measurements were also done. Making reference to results of these tests and giving attention to microscopic strain level induced by forced vibration tests, material properties for simulation analyses were determined as shown in Table 3. In evaluation of damping factors, results of regression analyses shown in Table 1 and Table 2 were also taken into consideration.

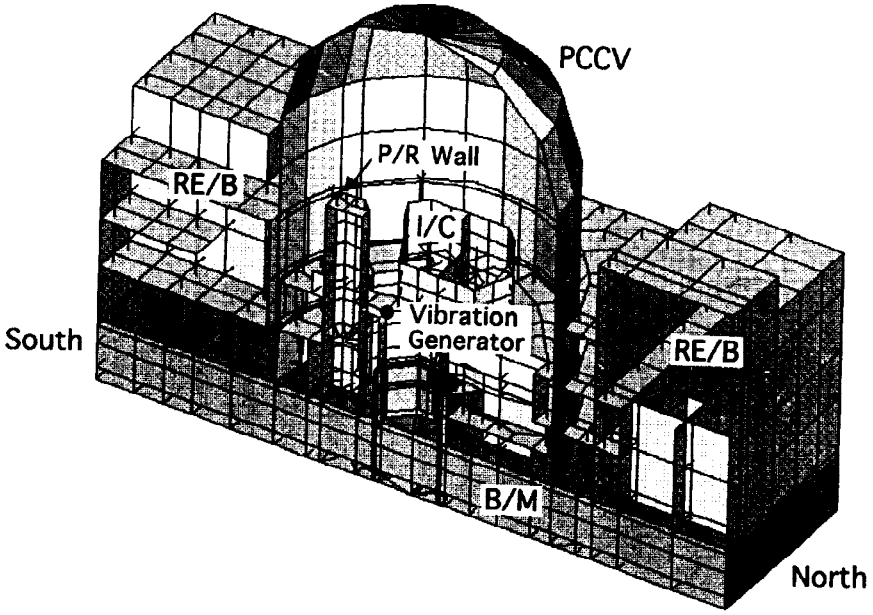

Fig.7. Outline of 3-D FEM model.

Table 3. Material properties of 3-D FEM model.

		Young's Modules	Poisson's Ratio	Damping Factor
PCCV		3.80×10^{6} (ton/m^2)	0.167	2 %
I/C, RE/B	Concrete	3.80×10^{6} (ton/m^2)	0.167	3 %
	Steel	2.1×10^{7} (ton/m^2)	0.300	1 %
Soil		1.2×10^{6} (ton/m^2)	0.373	2 %

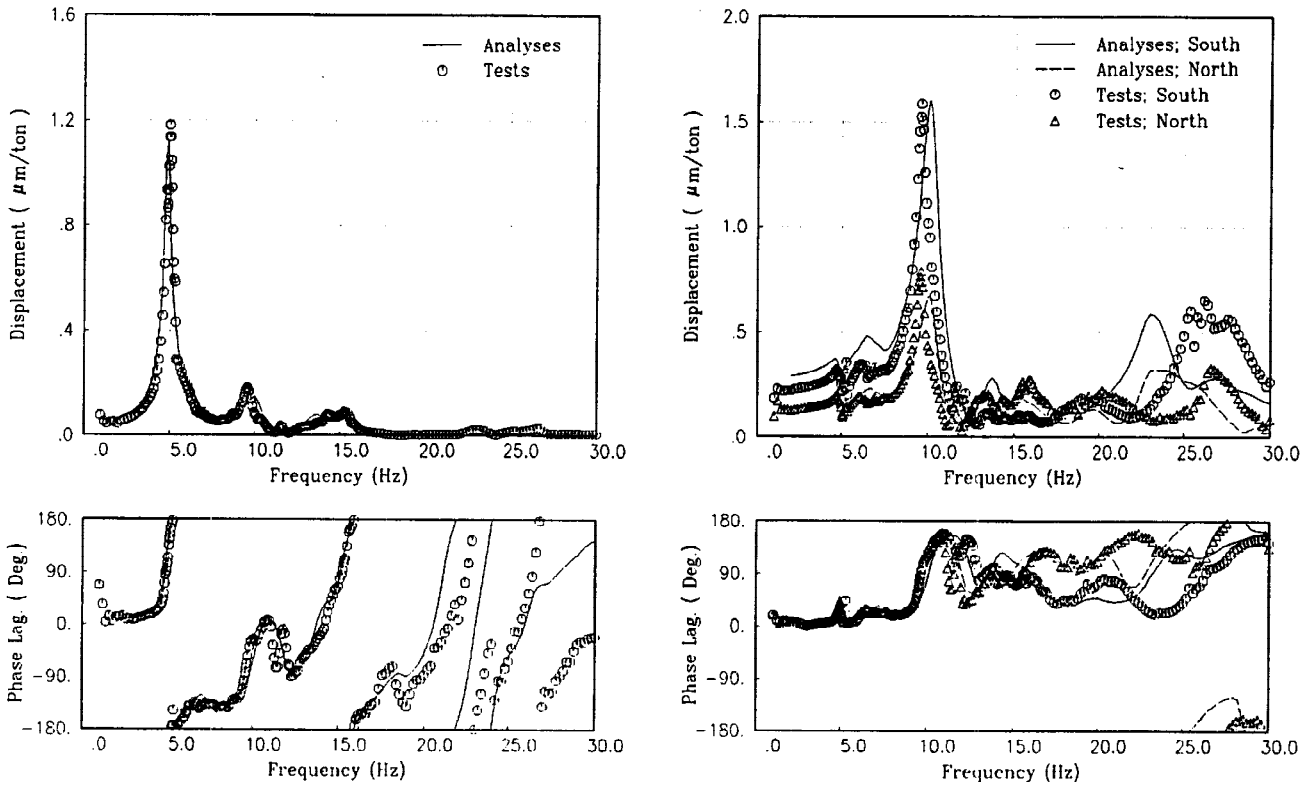

(a) PCCV (b) I/C

Fig.8. Resonance curves and phase lag curves from analyses and tests of I/C NS excitation.

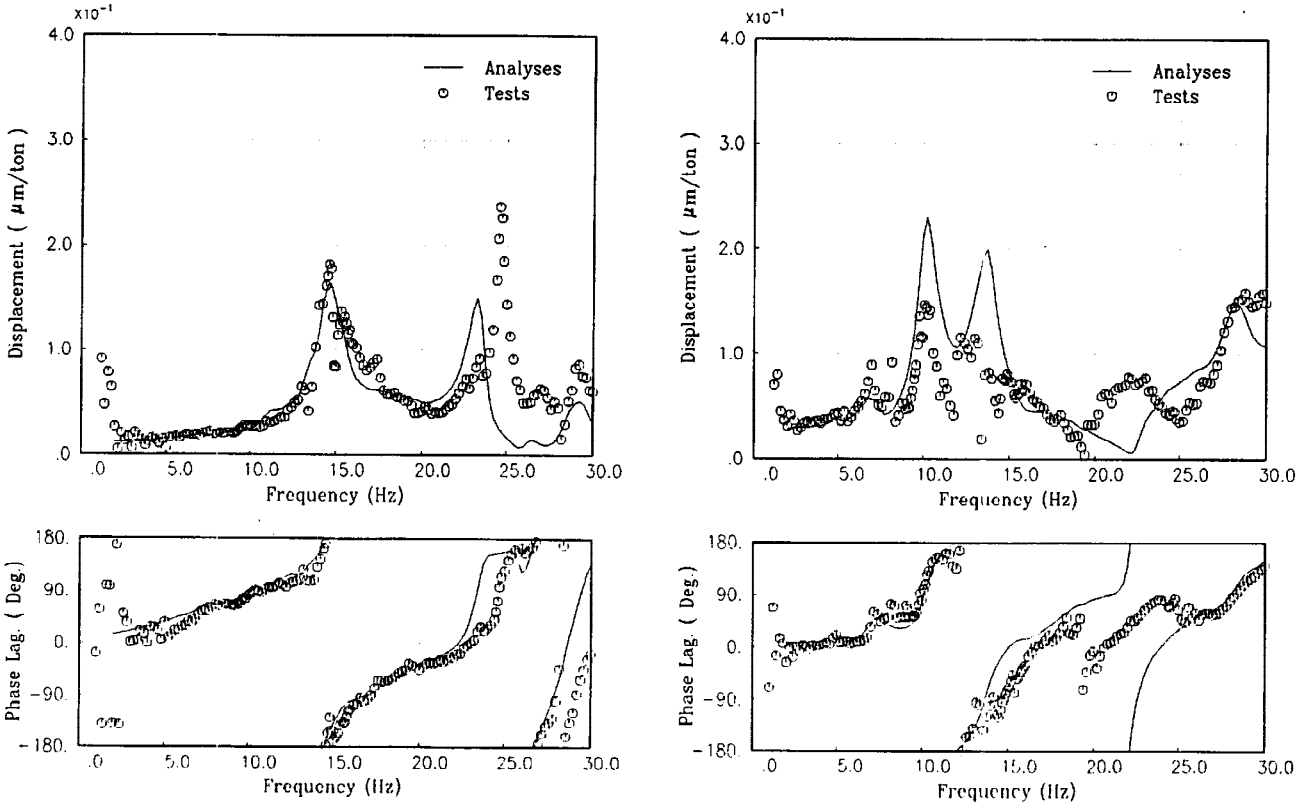

(a) PCCV (b) I/C

Fig.9. Resonance curves and phase lag curves from analyses and tests of I/C vertical excitation.

Analytical results

For I/C horizontal excitation, resonance curves and phase lag curves obtained from simulation analyses are shown in Fig.8. The solid line in Fig.8(a) represents results of the top of PCCV (EL+60.4m). The solid line and the dashed line in Fig.8(b) represent results of south side and north side of the operating floor of I/C (EL+11.3m), respectively. Results of tests, which are shown in Fig.2, are also drawn in Fig.8. From Fig.8(a) and Fig.8(b), it is observed that results of simulation analyses agree with those of tests. Similarly to the case of NS direction presented here, good agreements between results of simulation analyses and those of tests are observed in that of EW direction.

For I/C vertical excitation, resonance curves and phase lag curves obtained from simulation analyses were shown in Fig.9. The solid line in Fig.9(a) represents results of the top of PCCV (EL+60.4m). The solid line in Fig.9(b) represents results of south side of the operating floor of I/C (EL+11.3m). Results of tests, which are shown in Fig.4, are also drawn in Fig.9. From Fig.9(a) and Fig.9(b), it is observed that results of simulation analyses agree with those of tests.

Simulation analyses using 3-D FEM model have some advantages. For example, the vibration mode of the whole building is easily obtained by simulation analyses. As a representative sample, vibration mode at 14.6 Hz from I/C vertical excitation is shown in Fig.10. From this figure, it is observed that induced horizontal responses are more predominant than vertical ones at pressurized (P/R) wall. In addition, the horizontal displacement at the top of P/R wall is much larger than the vertical displacement at the top of PCCV. This feature is attributed to eccentricity of the placement of the vibration generator.

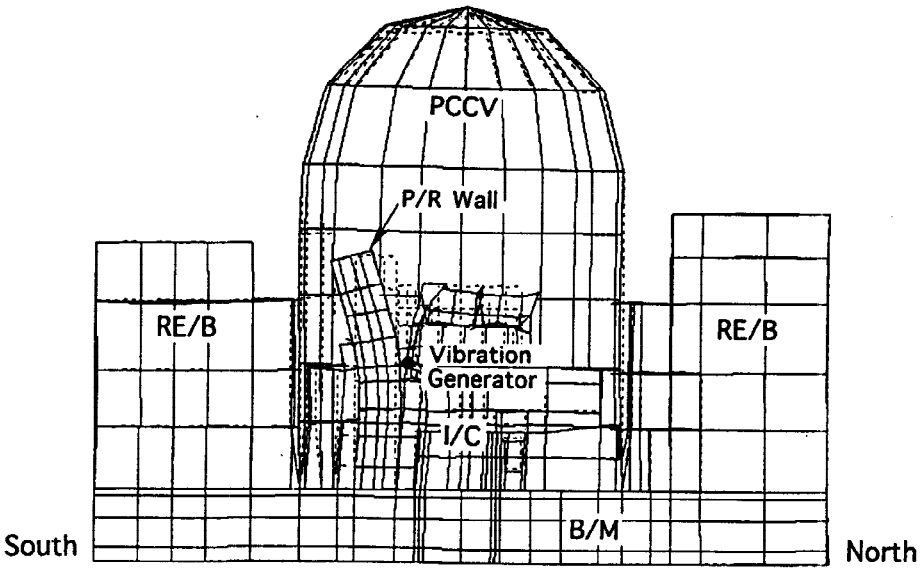

Fig.10. Modal shapes at 14.6 Hz from simulation of I/C vertical excitation.

CONCLUSION

3-D FEM model proved to be a useful tool to simulate forced vibration tests on vertical direction as well as those on horizontal directions. This remark suggests that better understanding of vibration characteristics of 3-D FEM model is required to make a reliable design model.